

# Study on dominant 2<sup>nd</sup> order nonlinear mechanism in AIN FBAR

AIN FBAR の支配的な 2 次非線形メカニズムに関する研究

Taisei Irieda<sup>1†</sup>, Tokihiro Nishihara<sup>1</sup>, Masanori Ueda<sup>1</sup>, and Ken-ya Hashimoto<sup>2</sup>  
(<sup>1</sup>TAIYO YUDEN CO., LTD.; <sup>2</sup>Grad. School Eng., Chiba Univ.)

入枝泰成<sup>1†</sup>, 西原時弘<sup>1</sup>, 上田政則<sup>1</sup>, 橋本研也<sup>2</sup> (<sup>1</sup>太陽誘電株式会社, <sup>2</sup>千葉大院 工)

## 1. Introduction

Suppression of nonlinear signal generation in radio frequency (RF) surface and bulk acoustic wave (SAW/BAW) devices is one of the most important subjects on the RF front-end module of recent cellular handsets. Therefore, clarification of nonlinear signal generation mechanisms in SAW/BAW devices is in strong demand.

To simulate nonlinear signal generation in RF-BAW devices, Hashimoto et al. proposed the thickness extensional mode 1D-perturbation analysis model [1]. This model is applicable to all piezoelectric nonlinearity with some coefficients representing the underlying nonlinear physics in RF-BAW devices.

In this work, we measure the 2<sup>nd</sup> harmonic response (H2) of the film bulk acoustic resonator (FBAR) and identify the dominant nonlinear coefficients by comparing the H2 produced by the Hashimoto model against the measured data. And we discuss the dominant 2<sup>nd</sup> order nonlinear mechanisms in AIN FBAR.

## 2. FBAR for Measurement

We measured a resonator that has the following physical parameters:

~2.5 GHz FBAR	
Resonance frequency $f_r$	: 2404 MHz
Anti-resonance frequency $f_a$	: 2476 MHz
Piezoelectric layer	: AIN 980 nm
Top and bottom electrodes	: Ru 190 nm/Ru 185 nm
Electrode area	: 13800 $\mu\text{m}^2$
Input power in H2 measurement:	+26 dBm

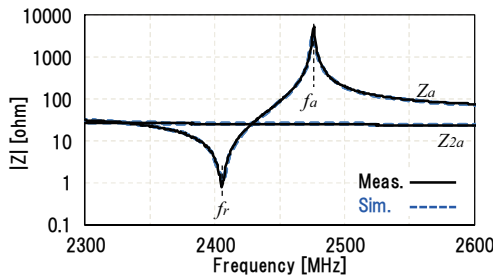


Fig. 1 Measured and simulated impedance  
Figure 1 shows measured impedance  $Z_a$  of the

resonator with the simulated one. Their agreement is well. In the figure, the simulated impedance  $Z_{2a}$  at the H2 frequencies is also shown. No acoustic resonance exists in  $Z_{2a}$  in this frequency range.

## 3. 2<sup>nd</sup> Order Non-Linear Coefficients

Following [1],  $h$ -form piezoelectric constitutive equations are used as follows:

$$T = c^D S - hD + T_N(S, D) \quad (1)$$

$$E = \beta^S D - hS + E_N(S, D) \quad (2)$$

where  $c^D$  is stiffness at constant  $D$ ,  $h$  is the piezoelectric constant, and  $\beta^S$  is the inverse permittivity at constant  $S$ .  $T_N$  and  $E_N$  in Eq. (1) and (2) are higher order terms given as a function of independent state variables  $S$  and  $D$  in the following forms up to the 2<sup>nd</sup> order:

$$T_N = -\frac{1}{2} \chi_{20}^T S^2 - \chi_{11}^T DS - \frac{1}{2} \chi_{02}^T D^2 \quad (3)$$

$$E_N = -\frac{1}{2} \chi_{11}^T S^2 - \chi_{02}^T SD - \frac{1}{2} \chi_{02}^E D^2 \quad (4)$$

The four constants  $\chi_{20}^T$ ,  $\chi_{11}^T$ ,  $\chi_{02}^T$ , and  $\chi_{02}^E$  in Eq. (3) and (4) are 2<sup>nd</sup> order nonlinear coefficients, and their major physical meanings are as follows:

---

$\chi_{20}^T$ :	strain dependent bulk modulus
$\chi_{11}^T$ :	strain dependent piezoelectric constant
$\chi_{02}^T$ :	electric flux dependent piezoelectric constant
$\chi_{02}^E$ :	electric flux dependent dielectric constant

---

## 4. Identification of Dominant 2<sup>nd</sup> Order Nonlinear Coefficient

We compared H2 simulation against measured data in the two following frequency ranges.

- Range I) 2300 MHz~2600 MHz
- Range II) 1150 MHz~1300 MHz

Range I) includes resonance and anti-resonance frequencies of the FBAR, and Range II) is half of Range I). Comparing in both frequency ranges can help to identify which nonlinear coefficient is dominant because the frequency patterns of state variables  $S$  and  $D$  change considerably in Ranges I) and II).

### 1) Single nonlinear coefficient

To identify which 2<sup>nd</sup> order nonlinear coefficient is dominant, first, we adjusted the value of each coefficient individually (with all other coefficients set to zero) until the simulated and measured H2 peaks were in agreement.

Figures 2 (a) and (b) show simulated and measured H2 in frequency Range I): (a)  $\chi_{20}^T$  is adjusted, and (b)  $\chi_{11}^T$  is adjusted. The agreement is well for both cases. Small notches below  $f_r$  in measured H2 are caused by transverse mode [2], and not concerned in this work. Although not shown here, the two remaining coefficients,  $\chi_{02}^T$  and  $\chi_{02}^E$ , cannot be adjusted because of the dip at  $f_a$ , which is not present in the measured data. From this,  $\chi_{20}^T$  or  $\chi_{11}^T$  is strong candidate for the dominant coefficient.

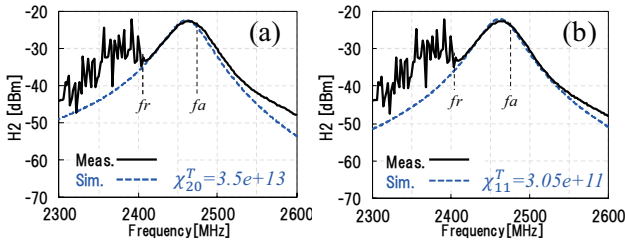


Fig. 2 Simulated and measured H2 in Range I)

Figure 3 shows simulated and measured H2 in Range II). Measured H2 show a dip around 1275 MHz. In this range, only  $\chi_{02}^E$  can be adjusted to reproduce the dip in Range II). Although the three remaining coefficients,  $\chi_{20}^T$ ,  $\chi_{11}^T$ , and  $\chi_{02}^T$ , can also give rise to H2, these H2 shapes are markedly different than the measurement (not shown here).

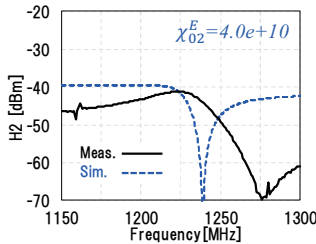


Fig. 3 Simulated and measured H2 in Range II) (only in case  $\chi_{02}^E$  shown here)

These results indicate that at least two non-zero nonlinear coefficients must be adjusted to be consistent with measured H2 in both frequency ranges simultaneously.

### 2) Two coefficient combinations

Next, we tried adjusting two coefficient combinations: (a)  $\chi_{20}^T$  and  $\chi_{02}^E$  and (b)  $\chi_{11}^T$  and  $\chi_{02}^E$ . Figures 4 (a) and (b) show these results. In Fig. 4 (a), the shape of H2 was a poor match to the measurement mainly because of two dips absent in the measured data in Range I). The simulated H2 shows notches because the H2 from  $T_N$  by  $\chi_{20}^T$  in Eq. (3) and  $E_N$  by  $\chi_{02}^E$  in Eq. (4) cancelled each other out.

On the other hand, in Fig. 4 (b), the shape of H2

was a good match to the data in both frequency ranges simultaneously. Therefore, we expect the combination of  $\chi_{11}^T$  and  $\chi_{02}^E$  to be the best candidate to explain how the second harmonic signal is generated. This combination indicates that the AlN layer in the FBAR has strain-dependent piezoelectricity and electric flux-dependent dielectricity nonlinear natures that dominate contributions to the 2<sup>nd</sup> harmonic response generation in the AlN FBAR.

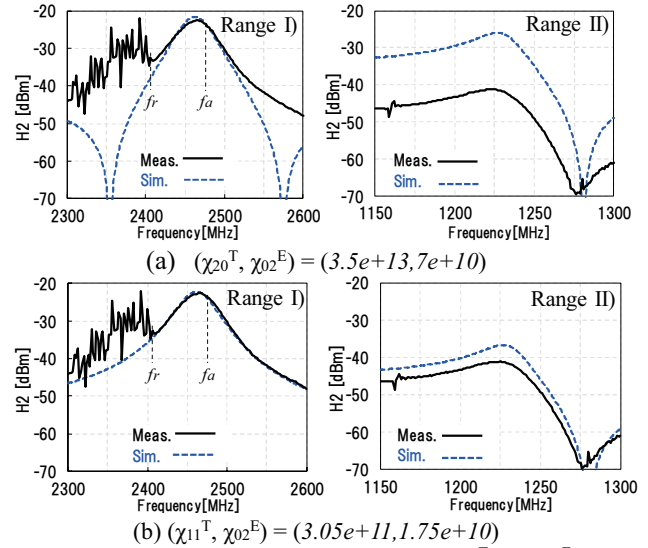


Fig. 4 Simulated and measured H2; (a)  $\chi_{20}^T$  and  $\chi_{02}^E$  are adjusted; (b)  $\chi_{11}^T$  and  $\chi_{02}^E$  are adjusted

In future work, we will verify these estimations and identify the dominant 3<sup>rd</sup> order nonlinear mechanism in the AlN FBAR.

## 6. Conclusion

In this paper, we investigated the dominant 2<sup>nd</sup> order nonlinear mechanism in the AlN FBAR.

We measured H2 in 2 frequency ranges, around  $f_r$  and  $0.5 * f_r$ , and adjusted the coefficients of the nonlinear simulation model to be consistent with measured H2 in both frequency ranges simultaneously.

As a result, combining  $\chi_{11}^T$  ( $= 3.05e+11$ ) and  $\chi_{02}^E$  ( $= 1.75e+10$ ) reproduced measured H2 behavior. This result indicates that strain-dependent piezoelectricity and electric flux-dependent dielectricity in AlN are the dominant underlying mechanisms of 2<sup>nd</sup> order nonlinear responses in the AlN FBAR.

## References

- [1] K. Hashimoto et al., (2017 EFTF/IFCS).
- [2] L. Qiu et al., USE2018 (2018) 3P3-9.